Population Transfer between Two Quantum States by Piecewise Chirping of Femtosecond Pulses: Theory and Experiment

S. Zhdanovich,[1,3] E. A. Shapiro,[2] M. Shapiro,[1,2,3] J. W. Hepburn,[1,2,3] and V. Milner[1,2,3]

[1]*Departments of Physics and Astronomy, The University of British Columbia, Vancouver, Canada*

[2]*Chemistry, The University of British Columbia, Vancouver, Canada*

[3]*The Laboratory for Advanced Spectroscopy and Imaging Research (LASIR), The University of British Columbia, Vancouver, Canada*

(Received 15 October 2007; published 13 March 2008)

We propose and experimentally demonstrate the method of population transfer by piecewise adiabatic passage between two quantum states. Coherent excitation of a two-level system with a train of ultrashort laser pulses is shown to reproduce the effect of an adiabatic passage, conventionally achieved with a single frequency-chirped pulse. By properly adjusting the amplitudes and phases of the pulses in the excitation pulse train, we achieve complete and robust population transfer to the target state. The piecewise nature of the process suggests a possibility for the selective population transfer in complex quantum systems.

DOI: 10.1103/PhysRevLett.100.103004 PACS numbers: 32.80.Qk, 42.50.Ct

The existence of robust and selective methods of executing population transfer between quantum states is essential for a variety of fields, such as precision spectroscopy and atomic clocks [1], quantum computing [2], control of molecular dynamics, and chemical reactions [3]. Traditionally, population transfer between two quantum states has been achieved by either executing a half-cycle Rabi oscillation, i.e., by applying a "π pulse," or by optically inducing an adiabatic passage (AP) between the states of interest [4]. Though the application of a π pulse can be implemented on a very short time scale, it is far from being robust, as it is highly sensitive to fluctuations in the laser power, phase, and pulse duration. In contrast, AP, which, for example, can be executed by the stimulated rapid adiabatic passage technique [5] or by slowly chirping the instantaneous frequency of the pulse, exhibits high degree of robustness against the fluctuations of many of the laser field parameters [4,5]. Because of this property, AP with chirped pulses has been widely employed for controlling atomic [6,7] and molecular [8,9] systems.

Though well suited for two-level systems, population transfer with chirped pulses in multilevel systems becomes sensitive to the exact value of the chirp and field strength [10,11], thus losing some of its appeal as a robust way of efficiently manipulating populations. When used with spectrally broad strong ultrashort pulses, frequency chirping can no longer selectively populate a prechosen superposition of states [9,11], and other methods of adiabatic [12] or nonadiabatic strong-field excitation must be employed. In the latter case, the problem can be treated in a purely empirical way by designing feedback-controlled experiments with genetic search algorithms [13,14]. Notably, the solution of Ref. [14] as well as the alternative approaches of strong-field population transfer [15,16] involve an accumulative action of sequences of laser pulses [17]. Yet the robustness and efficiency of the AP method has not been fully achieved.

Recently, we have demonstrated theoretically that one can implement AP with ultrashort pulses by executing the transfer of population in a piecewise manner [18,19]. The original work on piecewise adiabatic passage (PAP) [18] proposed using two temporally overlapping pulse trains. It was shown that one can bring about a complete population transfer between two quantum states through a third intermediate level. In this Letter we present the first experimental demonstration of the PAP method with a single pulse train by introducing the technique of "piecewise chirping." We show that the piecewise population transfer reproduces an AP process executed with a continuous frequency-chirped pulse, achieving comparable levels of robustness and efficiency.

Consider a system of two states, $|1\rangle$ and $|2\rangle$, of energies E_1 and E_2, driven by a near-resonant field with a frequency detuning Δ relative to the transition frequency $\omega_0 = (E_2 - E_1)/\hbar$. An arbitrary coherent superposition of these states can be written in the "laser" reference frame in terms of two angles, θ and ϕ, as

$$\psi = \cos\frac{\theta}{2}\exp\left[-i\frac{E_1}{\hbar}t\right]|1\rangle + \sin\frac{\theta}{2}\exp\left[-i\left(\frac{E_2}{\hbar} - \Delta\right)t + i\phi\right]|2\rangle.$$

This state can be represented as a unit Bloch vector pointing along the (θ, ϕ) direction. The rotating wave approximation results in two eigenstates, ψ_+ and ψ_-, which constitute two stationary points on the Bloch sphere, $(\theta_\pm, \phi_\pm)$. Here, $\tan\theta_\pm = \pm\Omega/\Delta$ and $\phi_\pm = \pm\pi/2$, Ω being the Rabi frequency. All other solutions of the time-dependent Schrödinger equation precess around the axes defined by the above stationary points, displaying periodic trajectories of the familiar Rabi oscillations [4].

In conventional AP with chirped pulses, Δ and Ω are slowly varied in time. If initially $\Delta \ll -|\Omega|$, and at the end of the process $\Delta \gg |\Omega|$, there is an interchange of pop-

ulations between state $|1\rangle$ and state $|2\rangle$. This is reflected on the Bloch sphere as a movement of the stable points from the $\theta = 0$ direction to the $\theta = \pi$ direction and vice versa. The above behavior holds as long as the adiabaticity condition is maintained:

$$|\dot{\theta}(t)| \ll \sqrt{\Delta^2(t) + \Omega^2(t)}. \quad (1)$$

In the "transition" frame, which rotates around the z axis with the angular velocity $\Delta(t)$ relative to the laser frame, the Bloch vector during AP proceeds via a spiral trajectory, as shown in Fig. 1(a) (see also Ref. [20]).

We now consider the evolution of the Bloch vector in the transition frame under the action of a train of short, mutually coherent, laser pulses. Each pulse, centered at the transition frequency ω_0 and of duration τ, generates a rotation $\hat{P} \equiv R(\alpha_P)$ of the Bloch vector by an angle $\alpha_P = \int_\tau \Omega(t)dt$ around an axis lying in the (x, y) plane. If the relative phase of the carrier oscillations of two pulses is zero, the corresponding rotation axes coincide. To account for the change in the carrier phase between consecutive pulses, instead of changing the rotation axis each time, we fix it along y but introduce an additional z rotation of the Bloch vector between the pulses, $\hat{F} \equiv R_z(\alpha_F)$. The overall evolution may be represented by a sequence of rotations $\hat{U} = \ldots \hat{F}\,\hat{P}\,\hat{F}\,\hat{P}\ldots$ The product $\hat{F}\,\hat{P}$ of two rotations is an overall rotation by an angle α_0 about an axis defined by the (θ_0, ϕ_0) angles, given to lowest-order expansion in α_P, α_F as

$$\alpha_0 = \sqrt{(\alpha_P^2 + \alpha_F^2)/2}, \quad (2)$$

$$\phi_0 = \pm\pi/2 - \alpha_F/2, \quad (3)$$

$$\tan\theta_0 = \pm\alpha_P/\alpha_F. \quad (4)$$

By maintaining the same value of α_F and α_P throughout the pulse train we induce piecewise rotations of the Bloch vector around the closest stable point (θ_0, ϕ_0). By slowly varying the values of α_P, α_F we can make the stable points move and the Bloch vector, captured near one of them, follow. Intuitively, the conditions of such piecewise following are: (i) the y and z rotations should be small (i.e., each pump pulse should induce an angular change much smaller than π and each increment in the carrier phase should be small too), and (ii) (θ_0, ϕ_0) should not move much from pulse to pulse, i.e.,

$$\Delta\theta_0 \ll \sqrt{(\alpha_P^2 + \alpha_F^2)/2}. \quad (5)$$

If initially $\alpha_P \ll |\alpha_F|$, the two stationary points, $\theta_0 = 0$ and $\theta_0 = \pi$, correspond to the bare states $|1\rangle$ and $|2\rangle$. As α_P increases and $|\alpha_F|$ decreases, the states originating in $|1\rangle$ and $|2\rangle$ move towards the equator of the Bloch sphere. They cross the equator as soon as α_F changes sign and finally interchange with each other. Depicted in the original transition frame, the trajectory of the Bloch vector is a piecewise spiral, as shown in Fig. 1(b).

The above analysis shows that the adiabatic following, similar to that implemented with the continuous chirped pulse, can be executed by a sequence of pulses with slowly varying amplitudes, and with the absolute carrier phase changing from pulse to pulse in a nonlinear way (i.e., decreasing α_F in the first half of the process and increasing α_F in the second). An example of such AP, corresponding to the piecewise population transfer in atomic Rb, is shown in Fig. 2. Here, the field is given by a sequence of 20 femtosecond pulses. For the kth pulse ($k \in [0, 20]$)

$$E_k(t) = A_k \cos[\omega_0 t + \Phi_k]\sin^2\left[\pi\frac{t - t_k}{\tau}\right], \quad (6)$$

where t_k marks the beginning of the kth pulse, with $\tau =$ 300 fs being its full duration. The A_k amplitude represents the train envelope parametrized as a Gaussian of 3 ps width (FWHM), and ω_0 is the transition frequency between the states $|1\rangle = 5s_{1/2}$ and $|2\rangle = 5p_{1/2}$ of Rb. The "piecewise chirp" of the pulse train is determined by the extra phase factor $\Phi_k = \bar{\alpha}(k - k_0)^2/2$, where $k_0 = 11$ and $\bar{\alpha} = 0.2$. As the pulse sequence proceeds, the pulse-to-pulse phase change, $\alpha_F = \bar{\alpha}(k - k_0) + \bar{\alpha}/2$, smoothly evolves from large negative values to large positive values. Our simulations show that as long as the conditions of piecewise adiabaticity (5) are maintained, the population transfer is

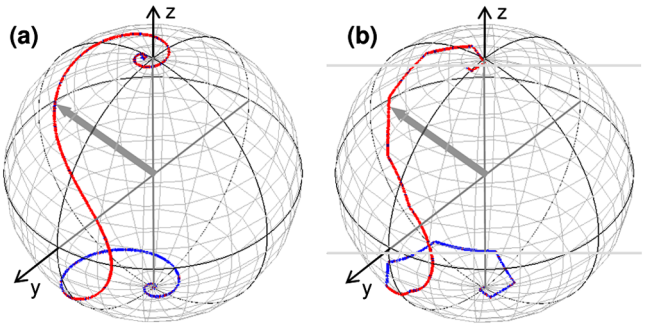

FIG. 1 (color online). Two calculated sample trajectories of the Bloch vector (thick gray arrow) during the AP process implemented in atomic Rb with a single continuous chirped pulse (a), and a train of 20 ultrashort pulses (b) (see text).

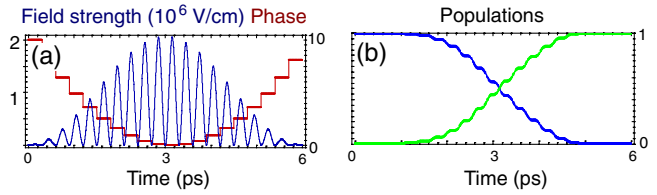

FIG. 2 (color online). (a) The amplitudes (oscillatory line, blue) and phases (piecewise parabola, red) of the driving field. (b) The populations of states $|1\rangle$ (falling, blue) and $|2\rangle$ (rising, green) during the PAP process.

robust with respect to the pulse shapes, their intensities, and the exact value of the piecewise chirp $\bar{\alpha}$.

The population transfer by piecewise chirping described here is a particular example of the piecewise adiabatic passage concept introduced in Ref. [18]. In the limit of infinitesimal rotations, the present process becomes equivalent to the usual continuous frequency chirping, associated with the quadratic phase change of the carrier phase in time. In this limit, the coarse-grained adiabaticity condition (5) reduces, up to a numerical factor, to the familiar quantum adiabaticity condition (1).

In the proof-of-principle experiment, we studied one-photon excitation of atomic rubidium (^{85}Rb) from the ground to the excited electronic state, $5s_{1/2}$ to $5p_{1/2}$, respectively. The effect of a single frequency-chirped laser pulse was compared with the effect of a short pulse train described above. The pulses were produced by a Ti:sapphire regenerative amplifier and had a spectral width of 7.1 nm (FWHM). We tuned the central wavelength of the laser to 795 nm, resonant with the $5s_{1/2} \rightarrow 5p_{1/2}$ transition. To generate a continuous or a piecewise chirp, the original pulse was spectrally shaped using a homemade pulse shaper based on a double-mask liquid crystal spatial light modulator in the $4f$ configuration [21]. The excitation beam was focused with a long focal length lens ($f =$ 100 cm) onto a cloud of rubidium atoms continuously evaporated from the rubidium dispenser in a vacuum chamber equipped with the time-of-flight ion detector.

To determine the population of the excited state, we ionized the atoms by a second probe pulse tuned to 1300 nm and arriving in the chamber 2.5 ps after the excitation pulse [Fig. 3(a)]. The ion signal provides good

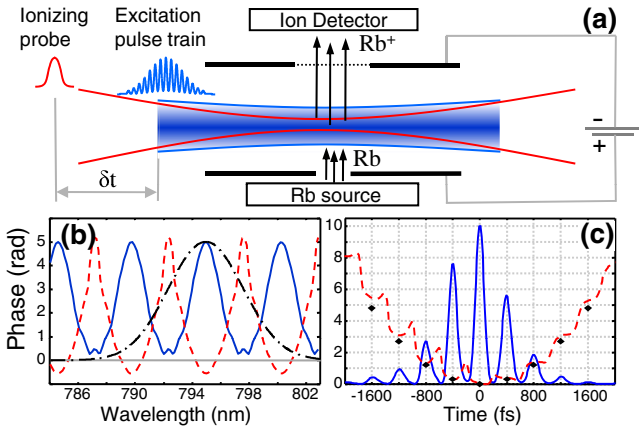

FIG. 3 (color online). (a) Experimental setup. Ion signal is measured for each excitation pulse (wide blue) followed by an ionizing probe (narrow red); (b) Amplitude (solid blue line) and phase (dashed red line) mask for generating a train of 9 pulses from a transform-limited pulse (dash-dotted black line). (c) FROG retrieval for the above pulse train with the temporal field amplitude (solid blue) and phase (dashed red), compared with the target quadratic phase of the pulses, Φ_k (black dots). All amplitudes are shown in arbitrary units.

selectivity between the ground and excited state Rb atoms because the ionization of $5s_{1/2}$ requires two more probe photons than that of $5p_{1/2}$. The power of the probe pulse was lowered to less than 0.1 μJ so as to produce no detectable ions from the atoms in the ground state. To ensure ion sampling from the region of uniform excitation field strength, we confined the interaction region in the longitudinal direction by a 3 mm aperture placed between the rubidium dispenser and the laser beam. We suppressed the transverse spatial averaging by focusing the probe beam to a smaller spot size than the size of the 795 nm beam ($1/e^2$ beam diameters of 180 and 470 μm, respectively). The effect of the laser power fluctuations was eliminated by recording the energy of each excitation pulse together with the corresponding ion count.

The resolution of our spectral pulse shaper of 0.17 nm per pixel allowed us to split the original pulse into a sequence of up to 9 well-separated pulses. Continuous chirping was applied by means of the quadratic phase-only modulation, $\phi(\omega) = \alpha(\omega - \omega_0)^2$, where α is the linear chirp and ω_0 is the center frequency of the pulse. Generation of a pulse train requires both the amplitude and phase modulation of the field spectrum. A sequence of N replicas of the original transform-limited pulse with the real amplitudes A_k and phases $\omega_0 t + \Phi_k$ separated by the time interval τ were obtained with the following complex spectral mask:

$$S(\omega_n) = \sum_k A_k e^{-i(k\omega_n \tau + \Phi_k)}/|S|, \tag{7}$$

where the frequency ω_n corresponds to the nth pixel of the pulse shaper, and the normalization factor $|S|$ was used to satisfy $|S(\omega_n)|^2 \leq 1 \forall\, n$. Examples of the applied spectral shaping and the corresponding pulse train, characterized by the method of frequency resolved optical gating (FROG), are shown in Figs. 3(b) and 3(c).

In Fig. 4 we show the measured ion count corresponding to the population of the $5p_{1/2}$ state of rubidium for various parameters of the excitation field. The oscillatory (blue) curve in plot (a) represents the well-known Rabi oscillations as a function of the energy of a single transform-limited pulse. This and all other experimental data points were normalized to the first maximum of this curve at around 0.1 μJ. Similar oscillatory dependence in plot (b) corresponds to the train of 7 pulses with Gaussian envelope of amplitudes and zero piecewise chirp, namely $A_k = \exp(-k^2 \ln 2/4)$ and $\Phi_k = 0$, where $-3 \leq k \leq 3$. The temporal separation between the pulses in the train was 400 fs. As expected, the integrated pulse area of the train is larger than the corresponding area of a single pulse with the same total energy. The difference stems from the different scaling of the pulse area and pulse energy with the field amplitude (first and second power, respectively), resulting in the smaller period of Rabi oscillations for the piecewise excitation.

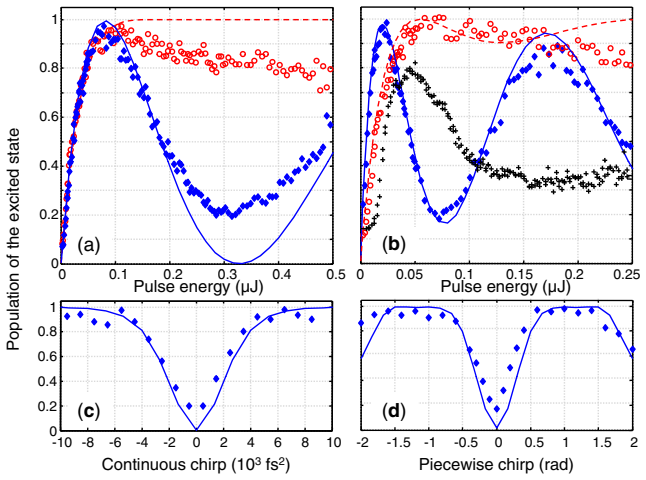

FIG. 4 (color online). Measured (dots) and calculated (lines) population of the excited state for a single pulse (a),(c) and a train of 7 pulses (b),(d). In (a) and (b), the efficiency of the population transfer is shown as a function of the integrated pulse energy. Blue diamonds and solid lines represent Rabi oscillations; red circles and dashed lines correspond to continuously (a) and piecewise (b) chirped excitation with $\alpha = 20 \times 10^3$ fs^2 and $\bar{\alpha} = 1$ radian, respectively. Black crosses in (b) represent an example of random distribution of phases Φ_k. In (c) and (d), the efficiency of the population transfer is shown as a function of the continuous and piecewise chirp, respectively. In both cases, the energy of the excitation field corresponds to the first minimum of the respective Rabi oscillation. Experimental signals on all four plots are normalized to the maximum of Rabi oscillations in plot (a).

When either continuous or piecewise chirp is applied to a single excitation pulse or a series of pulses, respectively, the amount of excited Rb atoms ceases to oscillate with the pulse energy. In both cases it saturates at the maximum value and becomes insensitive to the excitation field strength in the typical AP way [red circles in Figs. 4(a) and 4(b)]. We attribute the decay of both the amplitude of the Rabi oscillations and the saturated signal to the weak prepulse generated by our laser system 3 ns prior to the main pulse. To demonstrate the significance of the quadratic phase in the piecewise excitation, Fig. 4(b) also shows one example of the observed signal for a pulse train with randomly chosen Φ_k (black crosses). Different sets of random Φ_k produced different shapes of the energy dependence, but none of them resulted in the AP-like saturation of the population of the excited state close to the maximum value.

The stability of the adiabatic passage is reflected in the dependence of the transfer efficiency on the magnitude of the chirp. In both the continuous and piecewise scheme, we set the unchirped pulse area to 2π (energy of 0.31 and 0.07 μJ, respectively). The result of scanning the conventional chirp from -10^4 to $+10^4$ fs^2 is similar to scanning the piecewise chirp $\bar{\alpha}$ between -1.5 and $+1.5$ radians, attesting to the similar mechanisms of the two processes. Note the decay of the excited state population at $|\bar{\alpha}| > 1.5$ rad in plot (d), caused by the breakdown of the piecewise adiabaticity due to the increasingly high phase increments from pulse to pulse in the pulse train. Figure 4 also shows the results of numerical simulations. The only fitting parameter was the area of the excitation beam. FROG traces were used to define the temporal profile of the pulses.

Unlike the adiabatic transfer with continuously chirped pulses, PAP can be easily generalized to a wide class of cases. One can consider replacing states $|1\rangle$ or $|2\rangle$ by wave packets composed of many individual eigenstates, with the population transfer executed with a train of pulses separated in time by the wave packet's vibrational period. The ability to control the shape of the wave packet by shaping the pulses in the train positions PAP as a powerful tool in controlling molecular dynamics.

We thank A. Pe'er and J. Ye for valuable discussions and Q. Zhang for helping with the experimental setup. This work is supported by the CFI, BCKDF, and NSERC.

[1] S. A. Diddams *et al.*, Science **306**, 1318 (2004).
[2] M. A. Nielsen and I. L. Chuang, *Quantum Computation and Quantum Information* (Cambridge University Press, New York, 2000).
[3] M. Shapiro and P. Brumer, *Principles of the Quantum Control of Molecular Processes* (Wiley-Interscience, Hoboken, New Jersey, 2003).
[4] L. Allen and J. H. Eberly, *Optical Resonance and Two-Level Atoms* (Wiley, New York, 1975).
[5] N. V. Vitanov *et al.*, Adv. At. Mol. Opt. Phys. **46**, 55 (2001).
[6] B. Broers, H. B. van Linden van den Heuvell, and L. D. Noordam, Phys. Rev. Lett. **69**, 2062 (1992).
[7] B. Chatel *et al.*, Phys. Rev. A **68**, 041402(R) (2003).
[8] S. Chelkowski, A. D. Bandrauk, and P. B. Corkum, Phys. Rev. Lett. **65**, 2355 (1990).
[9] J. S. Melinger *et al.*, J. Chem. Phys. **101**, 6439 (1994).
[10] J. Cao, C. J. Bardeen, and K. R. Wilson, Phys. Rev. Lett. **80**, 1406 (1998).
[11] V. S. Malinovsky and J. L. Krause, Phys. Rev. A **63**, 043415 (2001).
[12] P. Kral, I. Thanopulos, and M. Shapiro, Rev. Mod. Phys. **79**, 53 (2007).
[13] R. S. Judson and H. Rabitz, Phys. Rev. Lett. **68**, 1500 (1992).
[14] C. Trallero-Herrero, J. L. Cohen, and T. Weinacht, Phys. Rev. Lett. **96**, 063603 (2006).
[15] N. Dudovich *et al.*, Phys. Rev. Lett. **94**, 083002 (2005).
[16] M. Wollenhaupt *et al.*, Phys. Rev. A **73**, 063409 (2006).
[17] A. Pe'er *et al.*, Phys. Rev. Lett. **98**, 113004 (2007).
[18] E. A. Shapiro *et al.*, Phys. Rev. Lett. **99**, 033002 (2007).
[19] E. A. Shapiro *et al.*, arXiv:0710.5502v1.
[20] M. Wollenhaupt *et al.*, Appl. Phys. B **82**, 183 (2006).
[21] A. M. Weiner, Rev. Sci. Instrum. **71**, 1929 (2000).